

# Phase structure and dynamics of dense QCD



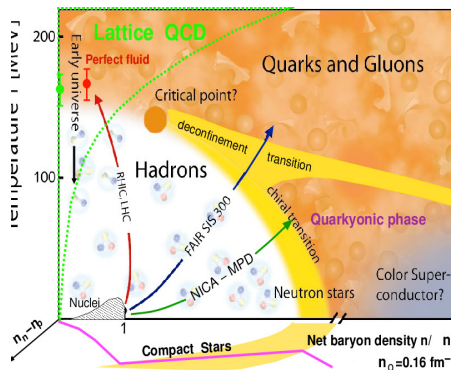
Armen Sedrakian

BNL Theory Seminar



Brookhaven National Laboratory, 18 November, 2016

- 1 Dense cold QCD, equation of state of color superconducting compact stars
- 2 Phase transitions, neutrino radiation and thermal cooling of neutron stars
- 3 Axion limits from astrophysics



Phase structure  
and dynamics  
of dense QCD

A Sedrakian

Introduction

Cold QCD and  
compact stars

Phase  
transitions in  
QCD and  
cooling  
transient in Cas  
A

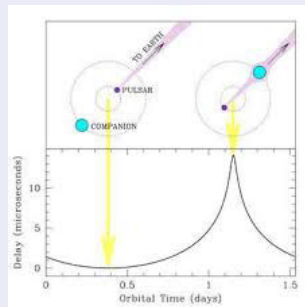
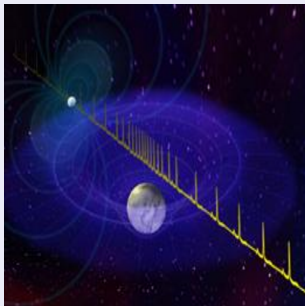
Axion cooling  
of NS

Thank you

## II. Cold QCD and compact stars

## A two-solar-mass neutron star measured

The largest pulsating star yet observed doubts on exotic matter theories



The binary millisecond pulsar J1614-223010+11 Shapiro delay signature:

$$\Delta t = -\frac{2GM}{c^3} \log(1 - \vec{R} \cdot \vec{R}'). \quad (1)$$

The pulsars mass  $1.97 \pm 0.04$  solar masses which rules out almost all currently proposed hyperon or boson condensate equations of state. (Demorest et al, 2010, Nature 467, 1081)

## Color-superconductivity within the NJL model

## Lagrangian of the model:

$$\begin{aligned}
\mathcal{L}_Q = & \bar{\psi}(i\gamma^\mu \partial_\mu - \hat{m})\psi + G_V(\bar{\psi}i\gamma^\mu\psi)^2 + G_S \sum_{a=0}^8 [(\bar{\psi}\lambda_a\psi)^2 + (\bar{\psi}i\gamma_5\lambda_a\psi)^2] \\
& + G_D \sum_{\gamma,c} [\bar{\psi}_\alpha^a i\gamma_5 \epsilon^{\alpha\beta\gamma} \epsilon_{abc} (\psi_C)_\beta^b] [(\bar{\psi}_C)_\rho^r i\gamma_5 \epsilon^{\rho\sigma\gamma} \epsilon_{rsc} \psi_\sigma^s] \\
& - K \{ \det_f [\bar{\psi}(1 + \gamma_5)\psi] + \det_f [\bar{\psi}(1 - \gamma_5)\psi] \},
\end{aligned}$$

- quarks:  $\psi_\alpha^a$ , color  $a = r, g, b$ , flavor ( $\alpha = u, d, s$ );
- mass matrix:  $\hat{m} = \text{diag}_f(m_u, m_d, m_s)$ ;
- other notations:  $\lambda_a, a = 1, \dots, 8$ ,  $\psi_C = C\bar{\psi}^T$  and  $\bar{\psi}_C = \psi^T C$ ,  $C = i\gamma^2\gamma^0$ .

## Parameters of the model:

- $G_S$  the scalar coupling and cut-off  $\Lambda$  are fixed from vacuum physics
- $G_D$  is the di-quark coupling  $\simeq 0.75G_S$  (via Fierz) but free to change
- $G_V$  and  $\rho_{\text{tr}}$  are treated as free parameters

QCD interactions are most attractive in color anti-triplet channel. For order parameter:

$$\Delta \propto \langle 0 | \psi_{\alpha\sigma}^a \psi_{\beta\tau}^b | 0 \rangle$$

- Antisymmetry in colors  $a, b$  for attraction
- Antisymmetry in spins  $\sigma, \tau$  for the BCS mechanism to work
- Antisymmetry in flavors  $\alpha, \beta$  to avoid Pauli blocking

Low densities and temperatures: 2SC phase

$$\Delta(2SC) \propto \Delta \epsilon^{ab3} \epsilon_{\alpha\beta} \quad \delta\mu \ll \Delta, \quad m_s \simeq 0.$$

Low-temperatures, large mismatch *inhomogeneous (crystalline)* 2SC phase

$$\Delta(CSC) \propto \Delta \epsilon^{ab3} \epsilon_{\alpha\beta}, \quad \delta\mu \sim \Delta, \quad m_s \neq 0.$$

High densities nearly massless  $u, d, s$  quarks: CFL phase

$$\Delta(CFL) \propto \langle 0 | \psi_{\alpha L}^a \psi_{\beta L}^b | 0 \rangle = -\langle 0 | \psi_{\alpha R}^a \psi_{\beta R}^b | 0 \rangle = \Delta \epsilon^{abC} \Delta \epsilon_{\alpha\beta C}.$$

Other options are less favorable energetically.

To generate a nuclear DFT start with the Lagrangian :

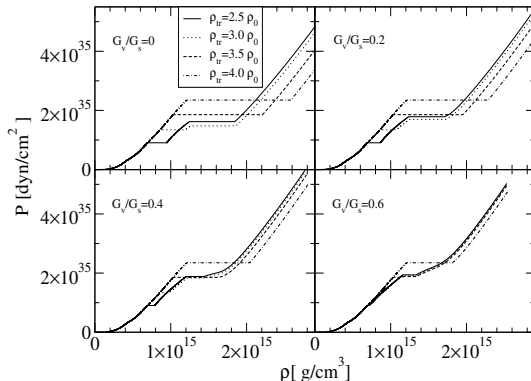
$$\begin{aligned}\mathcal{L} = & \sum_B \bar{\psi}_B \left[ \gamma^\mu \left( i\partial_\mu - g_{\omega BB} \omega_\mu - \frac{1}{2} g_{\rho BB} \boldsymbol{\tau} \cdot \boldsymbol{\rho}_\mu \right) - (m_B - g_{\sigma BB} \sigma) \right] \psi_B \\ & + \frac{1}{2} \partial^\mu \sigma \partial_\mu \sigma - \frac{1}{2} m_\sigma^2 \sigma^2 - \frac{1}{4} \omega^{\mu\nu} \omega_{\mu\nu} + \frac{1}{2} m_\omega^2 \omega^\mu \omega_\mu - \frac{1}{4} \boldsymbol{\rho}^{\mu\nu} \boldsymbol{\rho}_{\mu\nu} + \frac{1}{2} m_\rho^2 \boldsymbol{\rho}^\mu \cdot \boldsymbol{\rho}_\mu \\ & + \sum_\lambda \bar{\psi}_\lambda (i\gamma^\mu \partial_\mu - m_\lambda) \psi_\lambda - \frac{1}{4} F^{\mu\nu} F_{\mu\nu},\end{aligned}$$

- $B$ -sum is over the baryonic octet  $B \equiv p, n, \Lambda, \Sigma^{\pm,0}, \Xi^{-,0}$
- Meson fields include  $\sigma$  meson,  $\boldsymbol{\rho}_\mu$ -meson and  $\omega_\mu$ -meson
- Leptons include electrons, muons and neutrinos for  $T \neq 0$

- Assume the surface tension between nuclear and quark matter is high enough - no mixed phases and Maxwell construction can be applied
- Transition (deconfinement) occurs at some baryon chemical potential

$$P_N(\mu_B) = P_Q(\mu_B)$$

## EOS with equilibrium between nuclear, hypernuclear, 2SC and CFL phases of matter



- Phase equilibrium is constructed via Maxwell prescription
- Sequential phase transition  $NM \rightarrow 2SC \rightarrow CFL$

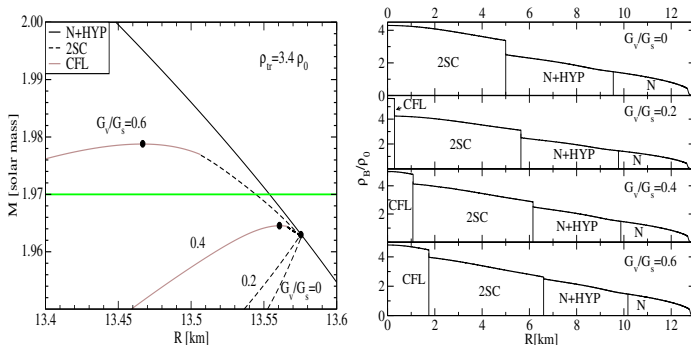
L. Bonanno, A. Sedrakian,

*Composition and stability of hybrid stars with hyperons and quark color-superconductivity.*

*Astronomy and Astrophysics* **539**, A16 (2012).



# Stability ( $M$ - $R$ diagram) and Internal structure of hybrid massive $\sim 1.9M_{\odot}$ star with color superconducting phases



- Small  $G_V$  2SC only. For large  $G_V$  CFL phase appears.
- Stability is achieved for  $G_V > 0.2$  and transition densities few  $\rho_0$



- To produce heavy and exotics featuring neutron stars it is sufficient to generate a stiff NM equation state above saturation.
- Vector interactions are mandatory to stabilize color superconducting quark stars.
- A  $2M_{\odot}$  mass star does not exclude exotic matter in the cores of NS
- Hyperonic sector requires also repulsive vector interactions or weakening of the  $\sigma$  exchange compared to SU(3) predictions
- Modifications of the gravity are also a possibility

- improvements in the range  $0.5 \leq \rho/\rho_0 \leq 2$  should be possible with the use of microscopically motivated models
- Quark matter EoS can be constrained at high densities by perturbative QCD results

L. Bonanno, A. Sedrakian,  
*Composition and stability of hybrid stars with hyperons and quark color-superconductivity.*  
Astronomy and Astrophysics **539**, A16 (2012).

G. Colucci, D. H. Rischke and A. Sedrakian,  
*Rotating hybrid compact stars.*  
Astron. and Astrophys. **559**, A118 (2013).

Phase structure  
and dynamics  
of dense QCD

A Sedrakian

Introduction

Cold QCD and  
compact stars

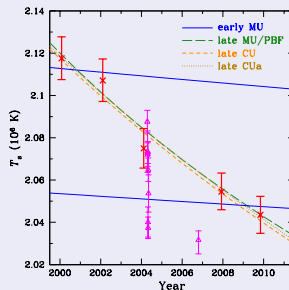
Phase  
transitions in  
QCD and  
cooling  
transient in Cas  
A

Axion cooling  
of NS

Thank you

### III. Phase transitions in QCD and cooling transient in Cas A

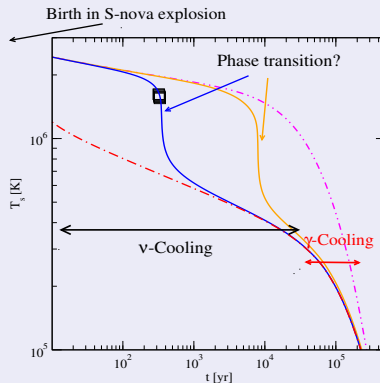
Chandra X-ray image of Cas A - the youngest (320 yr) SNR in the Milky Way.



NASA's Chandra X-ray Observatory has discovered the first direct evidence for a superfluid. Conclusions drawn from cooling simulations of the neutron stars.

The data has been doubted since. Possible instrumental contamination effects, obscuring of the star by passing cloud, geometrical effects

## Thermal history of Compact Stars (Cosmology in a single compact star)



$$\boxed{\frac{\partial S}{\partial t} + \vec{\nabla} \cdot \vec{q} = \mathcal{R} - \mathcal{L}_\nu - \mathcal{L}_\gamma} \quad dS = c_V dT, \quad \vec{q} = \kappa \vec{\nabla} T$$

- Dissipative function  $\mathcal{R} \propto \sigma(\nabla\phi)^2 + \kappa(\nabla T)^2/T + \dots$
- Neutrino losses  $\mathcal{L}_\nu$  from the bulk
- Photon losses  $\mathcal{L}_\gamma$  from the surface

- Modified Urca/brems process

$$n + n \rightarrow n + p + e + \bar{\nu},$$

$$n + n \rightarrow n + p + \nu + \bar{\nu},$$

- Crustal bremsstrahlung

$$e + (A, Z) \rightarrow e + (A, Z) + \nu + \bar{\nu},$$

- Cooper pair-breaking-formation

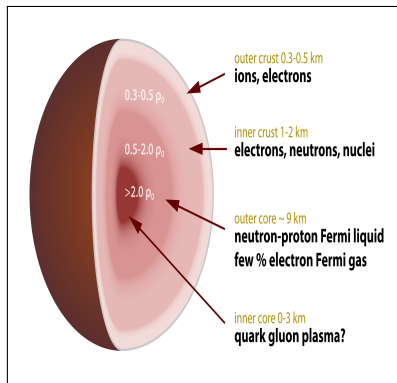
$$[NN] \rightarrow [NN] + \nu + \bar{\nu},$$

- Surface photo-emission

$$L_{\gamma} = 4\pi\sigma R^2 T^4$$

- Quark Urca process

$$d \rightarrow u + e + \bar{\nu}, \quad u + e \rightarrow d + \nu.$$



All axial vector neutral current process lead to axion emission

- $\nu$  and  $\bar{\nu}$  - Boltzmann equations with KB collision integrals

$$\left[ \partial_t + \vec{\partial}_q \omega_\nu(\vec{q}) \vec{\partial}_x \right] f_\nu(\vec{q}, x) = \int_0^\infty \frac{dq_0}{2\pi} \text{Tr} \left[ \Omega^<(q, x) S_0^>(q, x) - \Omega^>(q, x) S_0^<(q, x) \right],$$

- $\nu$ -quasiparticle propagators:

$$S_0^<(q, x) = \frac{i\pi \not{q}}{\omega_\nu(\vec{q})} \left[ \delta(q_0 - \omega_\nu(\vec{q})) f_\nu(q, x) - \delta(q_0 + \omega_\nu(\vec{q})) (1 - f_{\bar{\nu}}(-q, x)) \right].$$

- self-energies of neutrinos

$$-i\Omega^{>, <}(q_1, x) = \int \frac{d^4 q}{(2\pi)^4} \frac{d^4 q_2}{(2\pi)^4} (2\pi)^4 \delta^4(q) i\Gamma_{Lq}^\mu iS_0^<(q_2, x) i\Gamma_{Lq}^\dagger{}^\lambda i\Pi_{\mu\lambda}^{>, <}(q, x),$$

- energy loss per unit time and volume

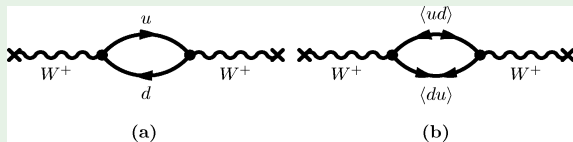
$$\epsilon_{\nu\bar{\nu}} = \frac{d}{dt} \int \frac{d^3 q}{(2\pi)^3} [f_\nu(\vec{q}) + f_{\bar{\nu}}(\vec{q})] \omega_\nu(\vec{q}) \quad (2)$$

- expressed through the collision integrals

$$\begin{aligned} \epsilon_{\nu\bar{\nu}} = & -2 \left( \frac{G}{2\sqrt{2}} \right)^2 \sum_f \int \frac{d^3 q_2}{(2\pi)^3 2\omega_\nu(\vec{q}_2)} \int \frac{d^3 q_1}{(2\pi)^3 2\omega_\nu(\vec{q}_1)} \int \frac{d^4 q}{(2\pi)^4} \\ & (2\pi)^4 \delta^3(\vec{q}_1 + \vec{q}_2 - \vec{q}) \delta(\omega_\nu(\vec{q}_1) + \omega_\nu(\vec{q}_2) - q_0) [\omega_\nu(\vec{q}_1) + \omega_\nu(\vec{q}_2)] \\ & g_B(q_0) [1 - f_\nu(\omega_\nu(\vec{q}_1))] [1 - f_{\bar{\nu}}(\omega_\nu(\vec{q}_2))] \Lambda^{\mu\lambda}(q_1, q_2) \text{Im} \Pi_{\mu\lambda}^R(q). \end{aligned}$$



## Polarization tensors at one loop



$$\Pi_{\mu\lambda}(q) = -i \int \frac{d^4 p}{(2\pi)^4} \text{Tr} [(\Gamma_-)_{\mu} S(p) (\Gamma_+)_{\lambda} S(p+q)]$$

with the input

$$\begin{aligned} \Gamma_{\pm}(q) &= \gamma_{\mu}(1 - \gamma_5) \otimes \tau_{\pm} \\ S_{f=u,d} &= i\delta_{ab} \frac{\Lambda^+(p)}{p_0^2 - \epsilon_p^2} (/p - \mu_f \gamma_0), \\ F(p) &= -i\epsilon_{ab3}\epsilon_{fg}\Delta \frac{\Lambda^+(p)}{p_0^2 - \epsilon_p^2} \gamma_5 C \end{aligned} \quad (3)$$

In the red-green color sector

$$\zeta = \Delta_{rd}/\delta\mu, \quad \delta\mu = (\mu_d - \mu_u)/2$$

and in the blue color sector

$$\Delta_b = 0 \quad \Delta_b \neq 0.$$

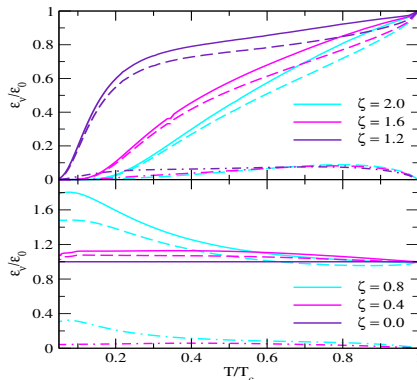
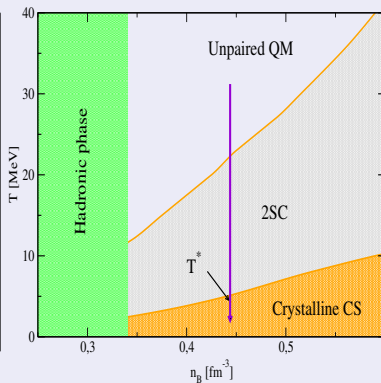
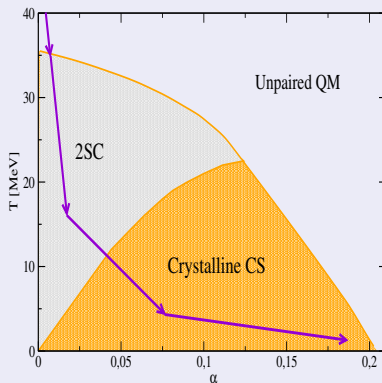


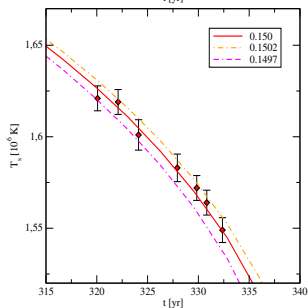
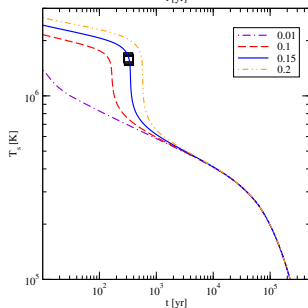
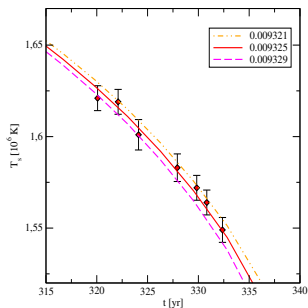
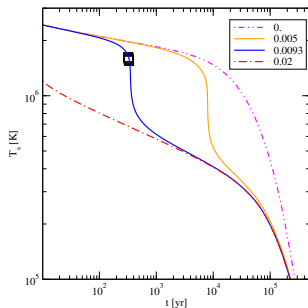
Figure : Upper panel: perfect 2SC phase  $\zeta > 1$ , Lower panel: crystalline phase  $\zeta < 1$

Phase transition within the QCD phase diagram can take place from one pairing pattern to the other (e.g. 2SC to Crystalline)



Left: Generic phase diagram of imbalanced fermi-systems; Right:  $\beta$ -equilibrated stellar matter

- 2SC phase - fully gapped, no excitations,  $\nu$ -emission strongly suppressed
- gapless (or crystalline) phase  $\nu$ -emission enhanced



Fine tuned to the Cas A data using the phase transition temperature  $T^*$  and  $\Delta b_{\pi}$

## Conclusions on Cas A transient

- At lower temperatures a transition from the BCS to a generic gapless phase must take place in the QCD phase diagram.
- We have modelled the emissivities of both phase in terms of a simple parameterization, which however takes into account the fact that as the temperature is lowered there is a phase transition from the 2SC to FF phase.
- The rapid cooling of the CS in Cas A can be accounted for via the phase transition described above. The Cas A data can be fitted by varying the phase transition temperature  $T^*$  at fixed value of the remaining physical parameters.
- Independent of the quality and correctness of the observational data, provided proof of principle that phase transitions may show up in transients in neutron star cooling evolution.

A. Sedrakian,

*Rapid cooling of Cassiopea A as a phase transition in dense QCD.*

Astron. and Astrophys. **555**, L10 (2013).

A. Sedrakian,

*Cooling compact stars and phase transitions in dense QCD.*

Eur. Phys. J. A **52**, 44 (2016).

Phase structure  
and dynamics  
of dense QCD

A Sedrakian

Introduction

Cold QCD and  
compact stars

Phase  
transitions in  
QCD and  
cooling  
transient in Cas  
A

Axion cooling  
of NS

Thank you

## IV. Axion cooling of NS

The origin of axions (Wilczek, Weinberg, 1978)

$$\mathcal{L}_{QCD} = \sum_q \bar{\psi}_q (iD - m_q e^{i\theta_q}) \psi_q - \frac{1}{4} G_{\mu\nu a} G_a^{\mu\nu} - \theta \frac{\alpha_s}{8\pi} G_{\mu\nu a} \tilde{G}_a^{\mu\nu} \quad (4)$$

The phase can be pushed in the last term by chiral rotation  $\psi'_q = e^{-i\gamma_5 \theta_q/2} \psi_q$

$$\mathcal{L}_{QCD} = \sum_q \bar{\psi}_q (iD - m_q) \psi_q - \frac{1}{4} G_{\mu\nu a} G_a^{\mu\nu} - \underbrace{(\theta - \arg \det M_q)}_{\bar{\theta}} \frac{\alpha_s}{8\pi} G_{\mu\nu a} \tilde{G}_a^{\mu\nu} \quad (5)$$

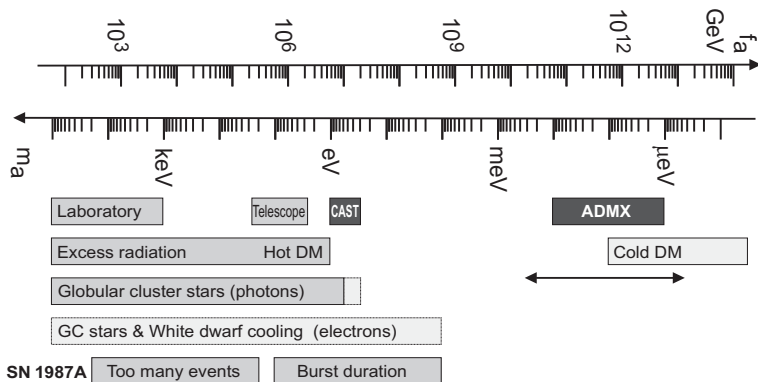
**Experimental value:**  $\bar{\theta} \leq 10^{-11}$  comes from neutron electric dipole moment

$$|d| = 0.63 \times 10^{-25} \text{ e cm} \quad (6)$$

**The strong CP problem - smallness of  $\bar{\theta}$  (unnatural).** Reinterpretation of  $\bar{\theta}$  term as a dynamical field pseudo-scalar axion field  $a(x)$  with decay constant  $f_a$

$$\mathcal{L}_{CP} = -\frac{\alpha_s}{8\pi} \bar{\theta} \text{Tr} G \tilde{G} \quad \rightarrow \quad \mathcal{L}_{CP} = -\frac{\alpha_s}{8\pi} \frac{a(x)}{f_a} \text{Tr} G \tilde{G} \quad (7)$$

The potential (mass term) forces the field to its minimum where  $\bar{\theta} = 0$ .





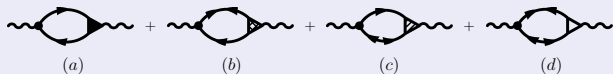
- Among the population of NS with measured surface temperature those that are warm are expected to have canonical masses  $M \sim 1.4M_{\odot}$ . (No exotic process are operating in their interiors). Thus, the physics of cooling is dominated by well-constrained nuclear physics of NS.
- Use a benchmark code (NSCool, D. Page) with standard input (APR EOS and gaps) to make results easy to check. (Note that in QCD part we use our own code tailored to treat quark matter phases, see [arXiv:1509.06986](https://arxiv.org/abs/1509.06986)).
- One single data point is sufficient to put a tight constraint on axion properties via cooling. We keep only data that is considered reliable (Cas A + several NS with age  $10^5$  yr).
- Among the continuum of models define by the coupling constants choose the most conservative ones  $C_e = 0$  (hadronic model of axions KVSZ).

- Most of the axion process relevant for NS cooling were computed by Iwamoto, Burrows 80's, Raffelt et al., Reddy et al in 90's
- First cooling simulations with axions in conference proceedings by Umeda, Tsuruta, Iwamoto in 1998 and then complete silence until 2015 [[arXiv:astro-ph/9806337](https://arxiv.org/abs/astro-ph/9806337)]
- Pair-breaking processes - J. Keller and A. S. (NPA, 2013) [[arXiv:1205.6940](https://arxiv.org/abs/1205.6940)]
- Full scale cooling simulations - A. S. (PRD, 2016) [[arXiv:1512.07828](https://arxiv.org/abs/1512.07828)]

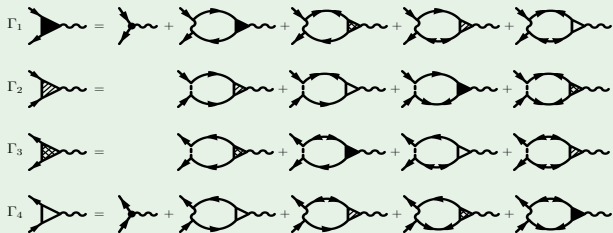
The neutrino emissivity is expressed in terms of the polarization tensor of baryonic matter

$$\varepsilon_{\nu\bar{\nu}} = -2 \left( \frac{G_F}{2\sqrt{2}} \right)^2 \int d^4 q g(\omega) \omega \sum_{i=1,2} \int \frac{d^3 q_i}{(2\pi)^3 2\omega_i} \text{Im}[L^{\mu\lambda}(q_i) \Pi_{\mu\lambda}(q)] \delta^{(4)}(q - \sum_i q_i),$$

Four polarization tensors in Nambu-Gorkov space:



Effective Bethe-Salpeter equations for vertices:

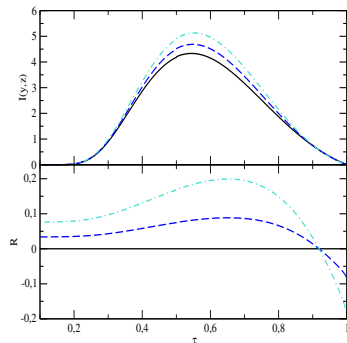


The vector current emissivity is given by

$$\epsilon = \frac{16G^2 c_V^2 \nu(0) v_F^4}{1215\pi^3} I(z) T^7,$$

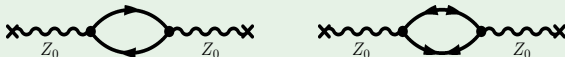
$$I(z) = z^7 \int_1^\infty \frac{dy y^5}{\sqrt{y^2 - 1}} f(zy)^2 \\ \times \left[ 1 + \left( \frac{7}{33} + \frac{41}{77} \gamma \right) v_F^2 \right].$$

$$z \equiv \Delta/T.$$



- Systematic expansion in  $v_F^2$ , leading order at  $v_F^4$
- The next-to-leading correction in  $v_F^2$  which is  $O(v_F^6)$  contributes about 10%.
- The emissivity has a maximum at  $\tau = T/T_c = 0.6$ , i.e., affects cooling close to the phase transition

Results due to Leinson-Perez (2006) Kolomeitsev-Voskresensky (2008) Reddy-Steiner (2008) A. S. et al (2007,2012)



The two diagrams contributing to the polarization tensor of baryonic matter, which defines the axial vector emissivity. The “normal” baryon propagators for particles (holes) are shown by single-arrowed lines directed from left to right (right to left). The double arrowed lines correspond to the “anomalous” propagators  $F$  (two incoming arrows) and  $F^+$  (two outgoing arrows).

The emissivity of this processes is given by

$$\epsilon_\nu = \frac{4G_F^2 g_A^2}{15\pi^3} \zeta_A \nu(0) \mathbf{v}_F^2 T^7 I_\nu, \quad I_\nu = z^7 \int_1^\infty dy \frac{y^5}{\sqrt{y^2 - 1}} f_F(z y)^2. \quad (8)$$

Note the  $v_F^2$  scaling of the axial neutrino emissivity compared to the  $v_F^4$  scaling.

Axial neutrino emissivity dominates the vector current emissivity because of  $v^2$  scaling instead of  $v^4$  scaling.

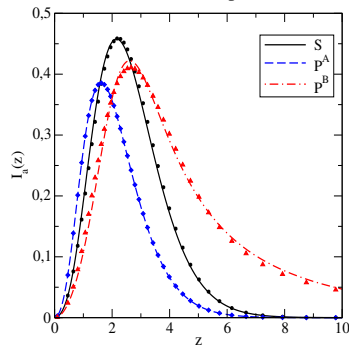


Key diagrams contributing to the axion pair-breaking emissivities are at one-loop level.

Axion emissivity for S-wave condensate

$$\epsilon_{aN}^S = \frac{2C_N^2}{3\pi} f_a^{-2} \nu_N(0) v_{FN}^2 T^5 I_{aN}^S,$$

$$I_{aN}^S = z_N^5 \int_1^\infty dy \frac{y^3}{\sqrt{y^2 - 1}} f_F(z_N y)^2.$$



J. Keller and A. S. (NPA, 2013) [arXiv:1205.6940] for S-wave condensate, A. S. (PRD, 2016) [arXiv:1512.07828] for P-wave condensates

The  $C_N$  charges are generally given by generalized Goldberger-Treiman relations

$$C_p = (C_u - \eta)\Delta_u + (C_d - \eta z)\Delta_d + (C_s - \eta w)\Delta_s, \quad (9)$$

$$C_n = (C_u - \eta)\Delta_d + (C_d - \eta z)\Delta_u + (C_s - \eta w)\Delta_s, \quad (10)$$

where  $\eta = (1 + z + w)^{-1}$ , with  $z = m_u/m_d$ ,  $w = m_u/m_s$ , and  $\Delta_u = 0.84 \pm 0.02$ ,  $\Delta_d = -0.43 \pm 0.02$  and  $\Delta_s = -0.09 \pm 0.02$ ,  $z = m_u/m_d = 0.35-0.6$ .

For *hadronic axions*,  $C_{u,d,s} = 0$ , and the nucleonic charges vary in the range

$$\boxed{-0.51 \leq C_p \leq -0.36, \quad -0.05 \leq C_n \leq 0.1.} \quad (11)$$

- neutrons may not couple to axions ( $C_n = 0$ )
- protons always couple to axions  $C_p \neq 0$
- **invisible axion DFSZ model**

$$C_e = \cos^2 \beta/3, \quad C_u = \sin^2 \beta/3, \quad C_d = \cos^2 \beta/3, \quad \text{arbitrary } \beta$$

- **KVSZ model  $C_e = 0$  and  $C_p$  and  $C_n$  from above inequalities**

The axion mass is related to  $f_a$  via the relation

$$m_a = \frac{z^{1/2}}{1+z} \frac{f_\pi m_\pi}{f_a} = \frac{0.6 \text{ eV}}{f_a/10^7 \text{ GeV}} \quad m_\pi = 135 \text{ MeV}, \quad f_\pi = 92 \text{ MeV}, \quad z = 0.56. \quad (12)$$

We now require that the axion luminosity does not exceed the neutrino luminosity

$$\frac{\epsilon_a}{\epsilon_\nu} = \frac{\alpha}{f_a^2 G_F^2 \Delta(T)^2} < 1, \quad (13)$$

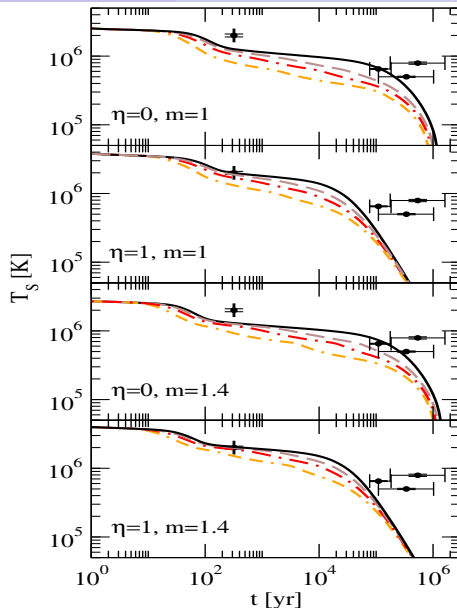
where we set the ratio  $I_a/I_\nu \simeq 1$  and find that  $\alpha \simeq 73.7$  ( $g_A = 1.25$ ). Our bound is given by (J. Keller and A. Sedrakian, Nucl. Phys. A, 897, 62, 2013)

$$f_a > 7.4 \times 10^9 \text{ GeV} \left[ \frac{0.1 \text{ MeV}}{\Delta(T)} \right], \quad (14)$$

which translates into an upper bound on the axion mass

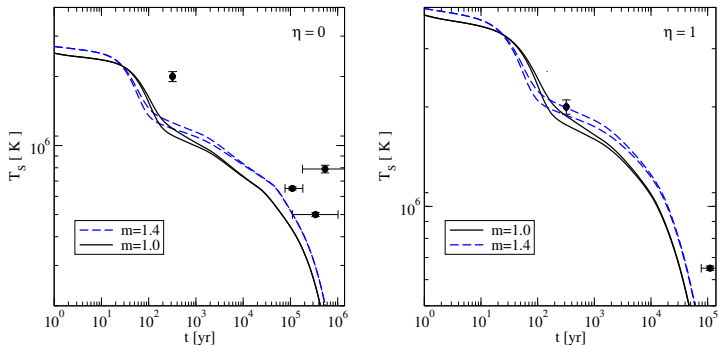
$$m_a = 0.62 \times 10^{-3} \text{ eV} \left( \frac{10^{10} \text{ GeV}}{f_a} \right) \leq 0.84 \times 10^{-3} \text{ eV} \left[ \frac{\Delta(T)}{0.1 \text{ MeV}} \right]. \quad (15)$$

The bound on  $f_a$  can be written in terms of the critical temperature by noting that  $\Delta(T) \simeq 3.06 T_c \sqrt{1 - T/T_c} \simeq T_c$  in the temperature range  $0.5 \leq T/T_c < 1$  of most interest.

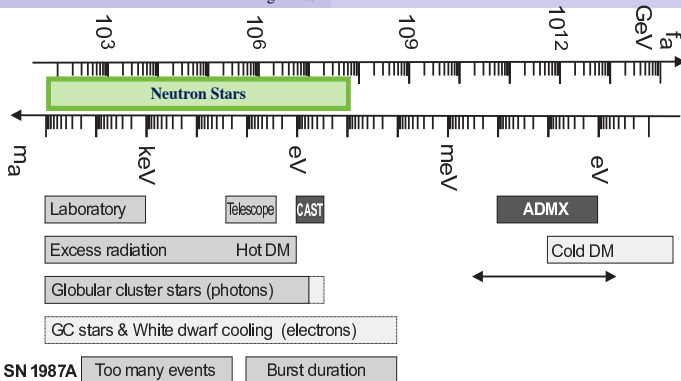


$f_{a7} = \infty$  (solid line) 10 (dashed), 5 (dash-dotted), and 2 (double-dash-dotted).





Cooling tracks of neutron star models with masses  $m = 1$  (solid) and 1.4 (dashed) for the case of a nonaccreted iron envelope ( $\eta = 0$ ) and accreted envelope ( $\eta = 1$ ) and for  $f_{a7} = 10$ . For each mass, the two tracks differ by the value of the neutron PQ charge. The upper curves correspond to our standard choice  $|C_n| = 0.04$ , while the lower curves correspond to the case of enhanced axion emission with  $|C_n| = |C_p| = 0.4$ .



The NS constraint are based on highly conservative physics of hadronic matter and on benchmarked code for cooling simulations of NS.

A. Sedrakian,  
*Axion cooling of neutron stars.*  
 Phys. Rev. D **93**, 065044 (2016).

J. Keller and A. Sedrakian,  
*Axions from cooling compact stars:  
 pair-breaking processes.*  
 Nuclear Physics A **897**, 62 (2013).

## Thanks to recent collaborators:

M. Alford

D. Rischke

A. Harutyunyan (grad. student)

X.-G. Huang

H. Nishimura

earlier work with: L. Bonanno, J. Keller

